THE 'HOW & WHY' A DECEPTIVELY SIMPLE ACOUSTIC RESONATOR BECAME THE BASIS OF A MULTI-BILLION DOLLAR INDUSTRY

Rich Ruby
Director of FBAR Technology, Fellow, Broadcom Ltd. San Francisco, USA

ABSTRACT

The ability to achieve ubiquitous connectivity and run powerful 'Apps' on today's Smart phones requires a front-end radio able to handle tremendous data rates; and that, requires access to the full bandwidth owned by service providers. Once, the front-end radio consisted of a single power amplifier (PA), filter/duplexer, a switch and a low noise amplifier (LNA). Early on, a cell phone might be able to access 2 or 3 frequency bands. Today, the iPhone 7 accesses 23 to 24 GSM, CDMA and LTE frequency bands, while the Galaxy flag ship phones from Samsung have 16 bands (not counting the GPS, Wi-Fi, Bluetooth and NFC radios).

Power amplifier, Low noise amplifier and switch functions can be combined –important for cost and size— but, proliferation of usable bands has driven up filter count. New bands are being created (opening up more frequency spectrum) and more challenging; existing bands are now being combined in what is called Carrier Aggregation. This requires better performance from the filter and also drives filters to become smaller as handset manufacturers struggle to add more filters into a limited space.

This has created (in just a few years) a whole new billion dollar industry focused on building high quality ultra-miniature filters; An industry where better quality filters enable better wireless communication, which -in turn- drives the technology to build better filters.

INTRODUCTION

A simple Process, A simple Model

The first miniaturized filters integrated into mobile devices were ceramic resonator/filters. But, their size precluded integrating more than one or two bands. In the early '90's, piezoelectric devices – literally microscopic acoustic resonators – were laid out in a half ladder topology consisting of series resonators and shunt resonators. Figure 1 is the measured duplexer (Tx/Rx) filter response using half-ladder topology for both filters. This product is in the front end radios for cell phones like the iPhone 7.

The first piezoelectric filters in cell phones used Surface Acoustic Devices (SAW) technology that required very little in the way of process complexity. Because of their process simplicity, SAW filters have come to dominate many of the low band frequency applications (< 1100 MHz). However, several fundamental weaknesses of this technology –especially in the mid and high band frequencies (1700 MHz to 6000 MHz), opened the door to Bulk Acoustic Devices (BAW). For a BAW device, the power handling, relative insensitivity to ESD (Electrostatic Discharge) and high intrinsic Q – relative to SAW, makes BAW filters ideal for the mid and high band filter applications.

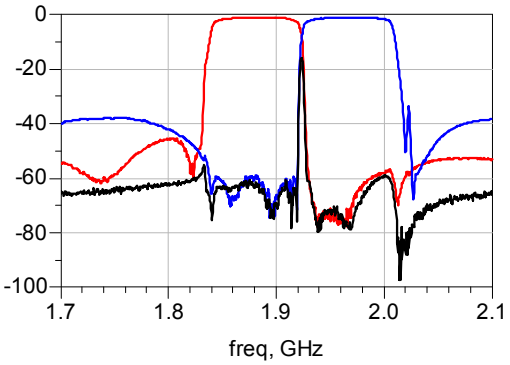

Figure 1: Typical pass band response of a duplexer (Tx and Rx filters). The red trace is the Tx passband, the blue trace is the Rx passband and the black line is the measured isolation between Tx and Rx

A simple process description of a BAW device would be a thin film dielectric (albeit with special properties) sandwiched between two thin film electrodes. This device is a capacitor and in any model of a BAW device, there is always a plate capacitance (C_o). However, the thin film dielectric must also have piezoelectric properties (the ability to convert electric fields into acoustic fields and back). There are several materials that lend themselves to thin film deposition techniques, Zinc Oxide (ZnO) and Aluminum Nitride (AlN). Of the two materials, AlN is the much preferred (although more difficult to reproduce reliably). The reason why AlN is better than ZnO would be higher Q, higher acoustic velocity, better temperature coefficient and relative acceptance into CMOS fabrication facilities [1,2].

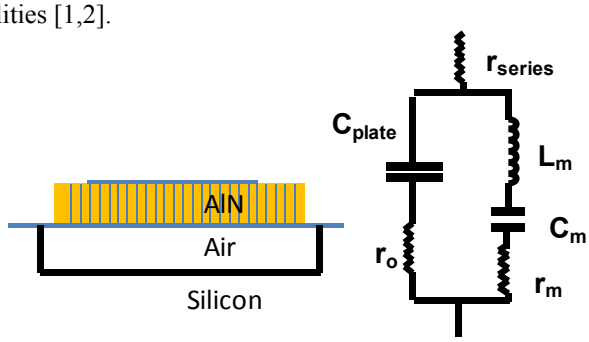

Figure 2a: A cross sectional drawing of an FBAR resonator. (2b) The modified Butterworth-Van Dyke model showing all 3 resistive losses

The next twist in the process is the de-coupling the 'capacitor' from the underlying substrate. There are two ways of accomplishing this; build up a series of low and high acoustic impedance films (e.g. tungsten /SiO2 paired thin films) that will create a Bragg mirror and solidly mount the 'capacitor' on top (Solidly Mounted Resonator or SMR-BAW [3]), or create a Free standing Bulk Acoustic Resonator (FBAR). The latter device can be created in one of several ways: First, etch material from

underneath starting from the back side of a substrate (a silicon substrate being ideal) or, a second way would be to create a 'pool' underneath the device, back fill with sacrificial layer (such as Phospho-Silica Glass or PSG) and then polish back using chemical mechanical polishing (CMP) to form a co-linear surface on which the resonator is deposited on [4]. Later in the process the sacrificial material is removed and a Free standing Bulk Acoustic Resonator (FBAR) is formed (Fig. 2a).

The model shown in Fig 2b is called the 'Modified Butterworth and Van Dyke' or mBVD model [5]. The model works amazingly well for designing FBAR filters. A simple L-R-C circuit in parallel with the plate capacitance, C_o, can represent the actual acoustic resonance. As long as a few rules are applied (e.g. the C_m / C_o ratio is fixed and the series resonance, f_s where $f_s = \left(2\pi * \sqrt{L_m C_m}\right)^{-1}$, an optimizer (in a commercial circuit simulator such as ADS[6]) can optimize a filter response. Higher Q means that the 3 loss resistors in Fig. 2b are smaller and thus the insertion loss is reduced and the roll-off or 'skirts' of the filter become steeper. There are 2 resonant conditions for an FBAR as seen on the Smith chart (Fig. 3a); the series resonance (mentioned above) and the parallel or anti-resonance defined as f_p and shown in Fig.3a.

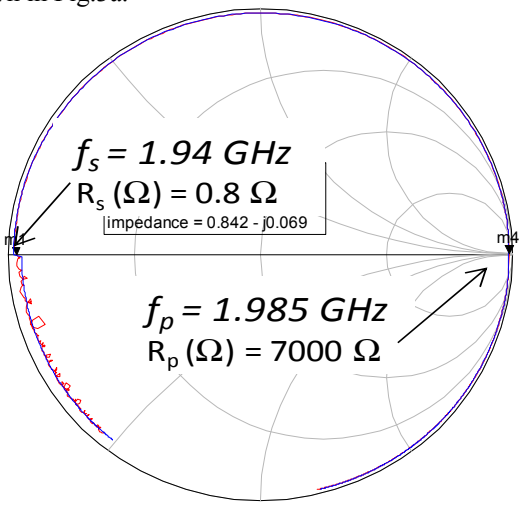

Figure 3a: S11 vs. frequency. Red is measurement, blue is the fit using the mBVD model.

The parallel resonance frequency, f_p , is higher due to the plate capacitance C_o being in series with the motional capacitance $C_m \rightarrow \frac{C_m C_o}{C_m + C_o}$. If the C_m / C_o ratio is small (typically < 10%) we can use a Taylor's series expansion for fp in terms of fs and write

$$f_p = f_p\left(1+0.5\frac{C_m}{C_o}\right) \quad or \quad \frac{f_p - f_s}{f_s} \approx 0.5*\left(\frac{C_m}{C_o}\right) \qquad (1)$$

Figure 3a is a measure of the reflected energy divided by the incident energy (as plotted on a Smith chart) and Fig 3b is a plot of the measured Q vs frequency. Landmarks, such as the series resonance and the parallel resonance along with the impedances R_s and R_p, are highlighted. One can write down the values of R_s and R_p in terms of the native impedance, X_o, of the resonator (as defined by the area, the piezoelectric material thickness d and the piezo dielectric constant).

$$R_s = r_s + r_m \quad R_p = X_o^2/(r_o + r_m) \quad X_o = (j\omega C_o)^{-1} \qquad (2)$$

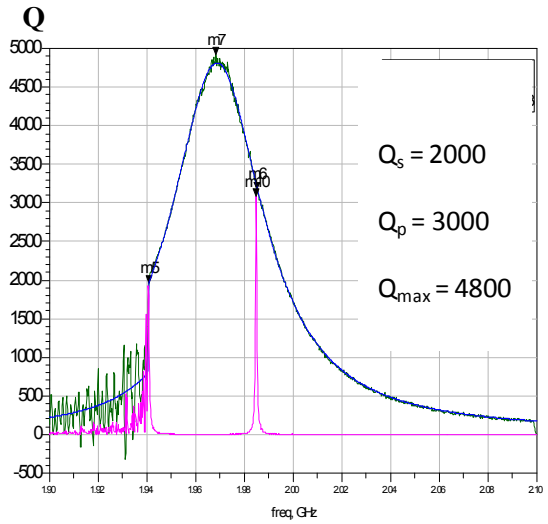

Figure 3b Plot of unloaded Q vs. frequency (green) for the Resonator shown in 3a. Q is also plotted against a fit (eq 10). Qs at fs, Qp at fp, and Qmax at fo are called out

A PHYSICAL MODEL

The model in Fig. 2b has no analogue to reality. Other than the plate capacitance, all the other terms in the mBVD model are merely electrical schematic representations of a ratio of polynomials. The cartoon cross section of the device shown does not reflect the thickness of the electrodes, their mass, their losses etc…

It is critical to understand the value of Q and the coupling coefficient of the piezoelectric layer. Understanding, measurement and careful monitoring of these two parameters in manufacturing will differentiate product quality and the ability to get design wins. Figure 4a represents a more realistic device cross section showing finite thickness electrodes, passivation etc.. The acoustic analog to this device is shown in Fig. 4b. An acoustic transmission line represents each layer in the 1-D model of the resonator, where the sound velocity and impedance of that segment can be described in terms of the stiffness coefficient c^E and mass density, ρ

$$v^a = \sqrt{c^E/\rho} \qquad Z_o^a = A*\sqrt{c^E \rho}$$

c^E is the 'unstiffened' stiffness coefficient (absence of electric field or absence of any piezoelectricity – the latter being the case for those acoustic transmission lines representing the finite thickness metal electrodes). Frequency dependent losses can easily be added to the

acoustic transmission lines or represented by external resistor terms (like the mBVD model) or both.

This model is referred to the Mason Model [7]. A transformer with a turns ratio of T:1, where T = $\sqrt{\left(\frac{k_t^2}{\pi}\right)\left(\frac{Z_{AlN}}{X_o}\right)}$ converts electrical impedance to acoustic impedance, is placed between the electrical response (output and plate capacitance C_o) and the internal acoustics of the resonator. Besides the transformer, the Mason model is noted for the necessity of creating a negative capacitor (here shown on the right side of the transformer) to cancel out the plate capacitance term in the acoustic regime.

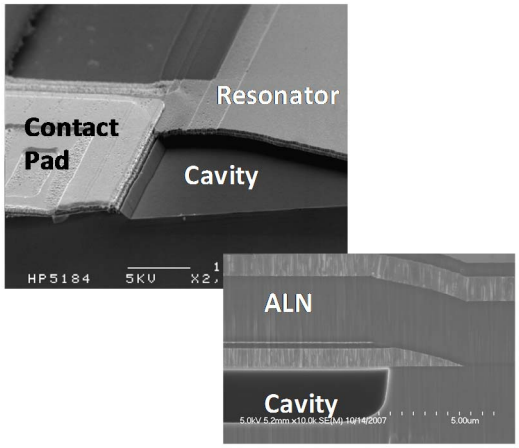

Figure 4a: SEM Micrograph of a partially exposed resonator spanning a silicon cavity. Inset is a close up of a zero drift resonator.

The acoustic model is an electrical representation of an acoustic phenomena first described by the constitutive equations that modify Gauss's law D= ε*E and Hooke's law $T=c^E$ *S, where stress T is units of N/m2 and c^E the stiffness constant with no electric field applied (or no piezoelectric properties) in units of N/m2 and the strain, S, is unitless.

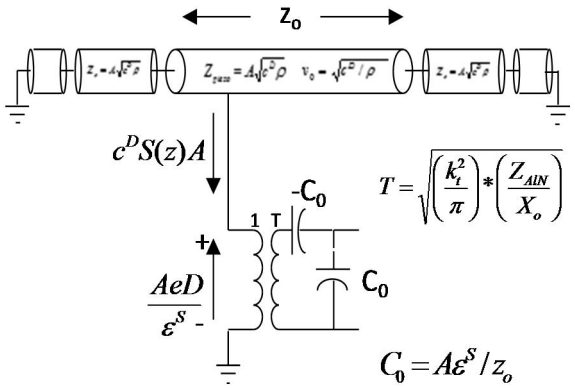

Figure 4b: The Mason model representation of an FBAR with finite thick electrodes and added passivation layers (A=Area).

In the equation below, e the piezoelectric constant is the same for both the E equation and the T equation…

$$\vec{E}(z) = \frac{\vec{D} - e\,S(z)}{\varepsilon} \qquad (3a)$$

$$T(z) = c^D\,S(z) - \frac{e\vec{D}}{\varepsilon} \qquad (3b)$$

Where $c^D = c^E + \frac{e^2}{\varepsilon}$ is the piezoelectric 'stiffened' stiffness coefficient. The displacement and electric field arrow notation will be dispensed moving forward.

For the rest of this analysis, we will assume infinitely thin electrodes in Fig 4a and b, thus the acoustic transmission line lengths representing the electrodes and other layers are set to zero.

At the parallel resonance, f_p, the electrical port is an open. Therefore the acoustic side of the transformer, A*e*D/ε where A = Area, must = 0. Since the two surfaces are free, the stress, T(±zo/2) must be zero. From Eq. 3b, $T=c^D$ S, therefore both S and T are zero at z=±zo/2. One can be write a solution for S and T as S = So cos(k_z*z) and T= To cos(k_z*z) where

$k_z = 2\pi f_p / v^a \qquad f_p = \frac{v^a}{2 z_o}$, and k_z is the wave number in the z direction at freq=f_p.

If there is finite piezoelectricity, there will be a series resonance (a short across the electrical port) at f_s.

There is a wave number, k_z', associated with fs, where k_z' will be smaller than k_z at f_p.

$$k_z' = k_z \frac{f_s}{f_p} = \frac{\pi}{z_o}\frac{f_s}{f_p} \qquad (4)$$

and the acoustic velocity is constant at both fs and fp.

Since the voltage across the electrodes (V=0),

$$V = \int_{-\frac{z_o}{2}}^{\frac{z_o}{2}} E\,dz = \frac{1}{\varepsilon}\int_{-\frac{z_o}{2}}^{\frac{z_o}{2}} (D - eS(z))\,dz = 0$$

or

$$z_o D = \int_{-\frac{z_o}{2}}^{\frac{z_o}{2}} eS(z)\,dz \qquad (5)$$

Substituting Eq. 5 back into Eq. 3b gives

$$T(z) = S_o c^D \cos(k_z' z) - \frac{e^2}{\varepsilon}\frac{S_o}{z_o}\int_{-\frac{z_o}{2}}^{\frac{z_o}{2}} \cos(k_z' z)\,dz$$

$$= S_o c^D \cos(k_z' z) - \frac{e^2}{\varepsilon}\frac{S_o}{z_o}\frac{2}{k_z'}\sin(k_z'\frac{z_o}{2}) \qquad (6)$$

Setting T(z=±zo/2)=0 at the two free surfaces at ±zo/2, one then gets

$$T(z=\pm\frac{z_o}{2})=0=S_o c^D \cos(k_z^{'}*\pm\frac{z_o}{2})-\frac{e^2}{\varepsilon}\frac{S_o}{z_o}\frac{2}{k_z^{'}}\sin(k_z^{'}\frac{z_o}{2})$$

giving

$$k_t^2 \equiv \frac{e^2}{\varepsilon\, c^D} = z_o \frac{k_z^{'}}{2}\frac{\cos(k_z^{'}\frac{z_o}{2})}{\sin(k_z^{'}\frac{z_o}{2})} \qquad (7)$$

where we define the intrinsic coupling coefficient $k_t^2 \equiv \frac{e^2}{\varepsilon\, c^D}$.

We can simplify eq. 7 and substituting eq. 4 we get

$$k_t^2 = \left(\frac{\pi}{2}\frac{f_s}{f_p}\right) \Big/ Tan\left(\frac{\pi}{2}\frac{f_s}{f_p}\right) \qquad (8a)$$

One can show that for $(f_p - f_s)/f_s$ < 6%, this transcendental equation can be simplified to

$$k_t^2 \approx \frac{\pi^2}{4}\frac{(f_p - f_s)}{(f_p + f_s)} \approx 2.4\,(f_p - f_s)/\,f_s \qquad (8b)$$

Going full circle back to eq. 1 we can equate k_t^2 to the Cm/Co ratio and we get.

$$k_t^2 \approx 1.2*\left(C_m \big/ C_o\right) \qquad (9)$$

In this simplified analysis, the coupling coefficient for a resonator assumed infinitesimally thin electrodes, and k_t^2 is the intrinsic coupling coefficient (the subscript "t" refers to the thickness or longitudinal mode). However, with finite electrodes, the coupling coefficient becomes $k_{t\,eff}^2$. It is the effective coupling coefficient that one gets from fp and fs in eq. 8 as read off a Q circle in Fig 3a.

Like the mBVD model, the Mason model can also be placed into an electrical schematic optimizer and the resonator elements (thickness, density of material, coupling coefficient etc…) can be optimized. The effective coupling coefficient, k_{teff}^2, will be altered by the addition of finite electrode and passivation layers to the piezo layer.

The three most important resonator properties are the electrical impedance, X_o, the effective coupling coefficient, k_{teff}^2, and the Q.

One can extract the unloaded Q from the measured Γ (or S11) in Fiq 3a. using the following equation[8].

$$Q(f)_{unloaded} = \frac{2\pi f \tau_g |\Gamma|}{1-|\Gamma|^2} \qquad (10)$$

Where the denominator represents the losses in the resonator and the numerator consists of the group delay, τ_g, frequency and the absolute value of the return loss, |Γ|. The group delay can also be written as $\tau_g \equiv \frac{\partial\phi}{\partial\omega} \approx \frac{\Delta\varphi}{\Delta\omega}$ and, when integrating from fs to fp on the Q circle, $\Delta\varphi \rightarrow \pi$ and w → 2π(fp –fs), one can re-write eq. 10 (letting f→ average of fs and fp, dropping terms like π and letting |Γ| → 1 and substituting fp-fs with kt2 from eq 8)

$$Q \approx \frac{1}{k_{teff}^2}\frac{1}{1-|\Gamma|^2} \quad or \quad k_{teff}^2 Q \approx \frac{1}{1-|\Gamma|^2}$$ Thus, one can get a sense of the Figure of Merit, $k_{teff}^2 Q$, as a function of the Q circle. The closer the Q circle is to the edge of the Smith Chart, the better the Figure of merit.

One can re-write Eq 2 (with Eq 8 and 9 and defining Q here as Q =ωL$_m$/r) for Rs and Rp as

$$R_p \cong 1.2 * X_o * (k_{teff}^2 Q) \qquad and \qquad R_s \cong 1.2 * X_o / (k_{teff}^2 Q)$$

As the Q circle gets closer to the edge of the Smith chart, $R_p \rightarrow \infty \quad and \quad R_s \rightarrow 0$.

Xo, the characteristic impedance of the resonator is set by the area and the thickness of the AlN film.

In practical filter designs, Xo centers around 50 Ohms for each of the resonators. The FoM had to be on the order of 50 to 100 for FBAR resonators (to be a viable compared to SAW devices). Starting from 'scratch' in the early '90's, it would seem unlikely that the FoM could be so high. Yet, some of the earliest resonators had k_{teff}^2 as high as 6% and Q's as high as 1500 to 2000. Today, we are achieving k_{teff}^2 as high as 9% and Q's on the order of 4000. A comparison of Q's, and Figure of Merit (FoM) for a variety of technologies including SAW devices, Lamb wave devices and MEMs devices is given in Ref [9].

The intrinsic coupling coefficient is limited to values around 10% for most practical devices today and set by the material parameters – the fundamental physics – of the piezoelectric. But, the Q is a variable where there is no known limit (although, again practically there will be a limit). Q can be divided into two types of loss mechanisms: bulk losses, i.e. losses associated with phonon scattering and thermo-elastic effects, and 'Anchor point' losses. Bulk losses depend on the quality of the deposited piezoelectric layer and the electrode layers. Anchor point losses have to do with acoustic energy that leaks out of the membrane and is not reflected or recovered. To minimize anchor point losses [10] a variety

of resonator design and process tricks are employed. Some, like adding frames around the perimeter helps to reflect acoustic energy that is the form of lateral modes get reflected back into the resonator and re-converted into the longitudinal mode [11].

Another 'trick' to improving the resonator performance is to 'apodize' the shape of the resonators such that any generated lateral modes will not find a natural resonant boundary condition created by two parallel edges. Figure 5 shows a layout of a typical FBAR filter.

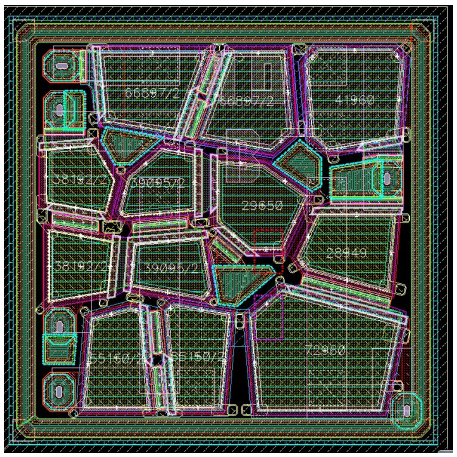

Figure 5: A Layout drawing of a typical FBAR filter. The non-Manhatten geometry helps 'smear' out strong lateral mode resonances created by parallel edges

The actual filter (as found in a phone) does not look anything like Fig. 5. This is because the filter is encased in an all-silicon package (we refer to this as microcap – a wafer scale package). A lid wafer which is used to seal the device consists of deep silicon vias, silicon treads (or 'knife edges') and silicon gaskets. The tread/gaskets (coated with gold) are mated to the base FBAR wafer using a gold-to-gold seal [12,13]. The tool technology for 'sculpting' the silicon lids came from the MEMs technology.

Figure 6 shows a packaged FBAR filter. The purpose of the package is to protect the resonator from any deleterious effects from the environment. Corrosion, absorption of moisture and even dust can cause the filters to shift in frequency.

One of the most stringent tests required by handset manufacturers is UHAST or Unbiased Highly Accelerated Stress Test. UHAST requires zero failures after 96 hours from 3 lots of 25 parts in 130C 85% humidity [14]. Failure of this test will result in a non-acceptance of your part. The gold on the lid wafer is patterned on the silicon gasket with 'knife edges' or treads to ensure hermetic sealing of the two wafers. The gasket and 'knife edges' are patterned and etched into the silicon. Deep vias on the lid wafer connect to the pads on the mating surface of the base wafer containing FBAR circuitry. The Deep silicon vias are then brought out to the top surface to either a bonding pad or more recently, copper pillars.

'DIVING' INTO THE PROCESS

Perhaps one of the luckiest 'hunches' was the idea that the electrodes should be made of molybdenum [15]. At the time, Au or Al were the only electrodes mentioned, yet, Au – a soft, ductile material—greatly degraded Q and Al, a very light material, did nothing for the k^2_{teff} and also degraded Q. Molybdenum and Tungsten, refractory metals, are extremely stiff, giving a high acoustic impedance, which helps trap the acoustic fields inside the piezoelectric layer [16] improving k^2_{teff} but, also greatly improving Q. Next, the chemistry was such that one could etch AlN without fear of etching into the bottom Mo (or W) electrode. Likewise, one could etch the top Mo (or W) electrode without fear of attacking the underlying AlN. The innate compatibility between AlN and Mo electrodes covered a multiplicity of processing 'challenges' created when using any other electrode material. In particular, k^2_{teff} uniformity, which is critical for today's filter designs. Lack of uniformity causes unacceptable variation in return loss.

The Q of the resonator is very dependent on the choice of materials and various process and design 'techniques' –much of which are trade secret and critical for differentiation. Again, uniformity of Q is important for yield. The roll-off (or 'skirts') defines the insertion loss at the edge of the band and the rejection/isolation out of band.

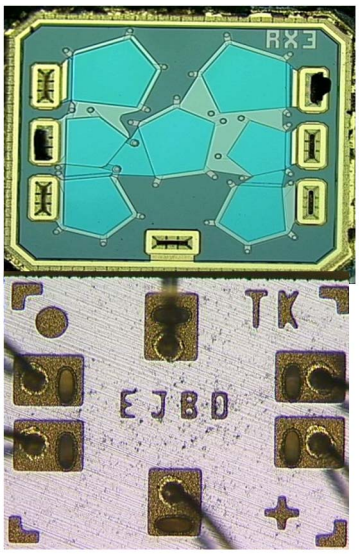

Figure 6: Optical photograph of the top surface of a microcap'd filter. The lid is hermetically sealed to an underlying FBAR die (top) with pads connected thru deep silicon etched vias. The markings on the gold pads are made by the etched 'knife edges' in the silicon gasket

For the 'tricky' process of de-coupling the FBAR from the underlying substrate, we created a depression or pool in the silicon substrate, back filled with a sacrificial layer (PSG) and then most important; polished the PSG such that the surface was co-linear with the silicon surface and was also atomically smooth. A simple dilute HF release of the low temperature deposited PSG is done near

the end of the process – freeing up the membrane [4].

The resonator was processed in such a way that after 'release', the resonator was anchored on all 4 sides, but the actual overlap between electrodes only occurred inside the 'pool'.

The choice and manner of preparation and deposition and patterning of electrodes, the method of de-coupling the substrate from the resonator, the method and tool choice for deposition of the piezoelectric and finally the hermetic package contribute to a strongly differentiated product. Although there have been many 'tweaks' to the process and process flow, it is a testament to the design of the FBAR process that in essence, the process flow has not materially changed in 20 years and the packaging, the microcap package, has not changed materially in 15 years.

CONCLUSION

For the Plenary talk, the paper and the talk will be quite different. The talk will focus more on the 'journey' and the paper is more of a tutorial tuned specifically to the descriptions and metrics needed to understand the development of FBAR. When this Author started an FBAR program at Hewlett Packard Labs in 1992/3, the dream was to see a product making millions of dollars. By early 2005, FBAR was selling tens of millions of filters and by 2010, many hundreds of millions of filters per year. By 2013/14 time frame, Avago/Broadcom crossed over the billion filters per year – and we continue to grow. What started out as 'outlier' project at HP Labs and cancelled more times that one would care to admit, is now a multi-billion dollar industry. The 'How' was starting out with the right formula for making high quality, robust filters with excellent manufacturing abilities. The 'Why' came about by the wholly unexpected demand for instantaneous communication and access to high volumes of data to one's personal cell phone.

ACKNOWLEDGEMENTS

REFERENCES

[1] K. Lakin, "Thin Film Resonators and Filters", *International Ultrasonic Symposium, pp.895-906, October 1999*

[2] R. Ruby, P. Bradley, J. Larson, Y. Oshmyansky, D. Figuredo, "Ultra-Miniature High-Q Filters and Duplexers Using FBAR Technology", in *Digest Tech. Papers Solid-State Circuits Conference* (ISSCC), San Francisco, Feb. 7, 2001

[3] R. Aigner, "SAW and BAW Technologies for RF Filter Applications: A Review of the Relative Strengths and Weaknesses", *International Ultrasonic Symposium.*, pp. 582-589, October 2008

[4] R. Ruby, Y. Desai, D. Bradbury, *SBAR Structures and Method of Fabrication of SBAR. FBAR Film Processing Tehcniques for the Manufacturing of SBAR/BAR Filters, ,* US Patent # 6,060,818 , May 2000

[5] J. Larson, P. Bradley, S. Wartenberg, R. Ruby,, "Modified Butterworth-Van Dyke Circuit for FBAR Resonators and Automated Measurement System", *International Ultrasonic Symposium*, pp. 863-868, October 2000.

[6] Advanced Design System (ADS), *Electronic Design Automation Software*, Product of KeySight Technologies

[7] W. P. Mason, *Piezoelectric Crystals and Their Applications to Ultrasonics*, D. Van Nostrand, 1950

[8] D. Feld, R. Parker, R. Ruby, P. Bradley,"After 60 Years: A New Formula for Computing Quality Factor is Warranted*", International Ultrasonics Symposium*, pp. 431-435, Oct. 2008

[9] R. Ruby, R. Parker, D. Feld, "Method of Extracting Unloaded Q Applied Across Different Resonator Technologies", *International Ultrasonics Symposium*, pp. 1815-1818, Oct. 2008

[10] R. Ruby, J. Larson, C. Feng, S. Fazzio, "The Effect of Perimeter Geometry on FBAR Resonator Electrical Performance", *IEEE Microwave Theory and Techniques Society Conference,* May 2005

[11] J. Kaitilya, M. Ylilammi, J. Ella, R. Aigner, "Spurious Resonance Free Bulk Acoustic Wave Resonators", *International Ultrasonic Symposium,* pp. 84-87, October 2003

[12] R. Ruby, T. Bell, F. Geefay, Y. Desai, *Microcap Wafer-Level Package with Vias,* US Patent # 6,228675, May 2001

[13] R. Ruby, A. Barfknecht, C. Han, Y. Desai, F. Geefay, G. Gan, M. Gat, T. Verhoeven, "High-Q FBAR Filters in a Wafer-Lvel Chip-Scale Package", in *Digest Tech. Papers Solid-State Circuits Conference* (ISSCC), San Francisco, Feb. 7, 2002

[14] **JEDEC Standard JESD47G** as created by the JEDEC Solid State Technology Association

[15] R. Ruby, P. Merchant, *Tunable Thin Film Acoustic Resonators and Method for Making Same,* US Patent # 5,587,620 , Dec. 1996

[16] K. Lakin, J. Belsick, J. McDonald, K. McCarron, "Improved Bulk Wave Resonator Coupling Coefficient for Wide Bandwidth Filters" *International Ultrasonic Symposium,* pp. 827-831, Oct 2001